Supporting Information

Ultrafine Pd_3Pb Intermetallic Nanowires with Mott Schottky effect Achieves Complete Oxidation Pathway for Methanol Oxidation Catalysis

Shuanglong Zhou[a], Zuochao Wang[a], Mo Zhang[b], Xiaoming Mou[c], Yu Dai[d], Lei Wang[a] and Jianping Lai[a,*]

[a] Key Laboratory of Eco-Chemical Engineering, Key Laboratory of Optic-electric Sensing and Analytical Chemistry of Life Science, Taishan Scholar Advantage and Characteristic Discipline Team of Eco-Chemical Process and Technology, College of Chemistry and Molecular Engineering, Qingdao University of Science and Technology, Qingdao 266042 (China)

[b] Xiamen Key Laboratory of Rare Earth Photoelectric Functional Materials, Xiamen Institute of Rare Earth Materials, Haixi Institute, Chinese Academy of Sciences, Xiamen 361021 (China)

[c] Analytical & Testing Center, Qingdao University of Science and Technology, Qingdao, 266042 (China)

[d] College of Foreign Languages, Qingdao City University, Qingdao 266106 (China)

Shuanglong Zhou, Zuochao Wang and Mo Zhang contributed equally to this work.

*Corresponding author.

E-mail addresses: jplai@qust.edu.cn (J. Lai)

Direct methanol fuel cell test

A membrane electrodes assembly (MEA) were prepared with 20 wt% commercial Pt/C and Pd_3Pb IM/MNC as anode and cathode, respectively. The loading amounts of commercial Pt/C and Pd_3Pb IM/MNC on 1.1 × 1.1 cm^2 electrode were 1.5 mg and 2 mg, respectively. MEA was prepared at 150 ℃ with a hot press impact of 70 kg/cm^2 for 120 seconds. Nafion 115 membrane is used to separate the anode and cathode. The assembled MEA was activated for 3 hours before testing. MEA was tested at 70 °C and the flow rates of methanol and oxygen were 1.5 mL/min and 150 mL/min, respectively.

In-situ FTIR test

The intermediate products during the MOR process were detected by *in-situ* FTIR through Thermo iS50 FT-IR with a liquid-nitrogen-cooled MCT-A detector. The in-situ FTIR curves were collected by the method of internal reflection. Firstly, the catalysts modified silicon crystal plated with gold was used as working

electrode, Ag/AgCl and Pt wire were worked as reference electrode and counter electrode respectively. All the tests were conducted in N_2 saturated 0.1 M KOH with 0.5 M methanol. The applied potential was stepped positively from 0.1 V to 1.2 V (*vs.* RHE) with an interval of 100 mV. Secondly, the results of in-situ FTIR were reported as relative change in absorbance: $\Delta R/R = (R(ES)-R(ER))/R(ER)$. The R(ES) and R(ER) are the spectra collected at the applied potential and reference potential (0.1 V *vs.* RHE). The upward bands represent the formation of products, the downward bands represent the consumption of reactants.

DFT calculation

The present first principle DFT calculations are performed by Vienna Ab initio Simulation Package (VASP) with the projector augmented wave (PAW) method. The exchange-functional is treated using the generalized gradient approximation (GGA) of Perdew-Burke-Emzerhof (PBE) functional. The energy cutoff for the plane wave basis expansion was set to 450 eV and the force on each atom less than 0.05 eV/Å was set for convergence criterion of geometry relaxation. Grimme's DFT-D3 methodology was used to describe the dispersion interactions. Partial occupancies of the Kohn−Sham orbitals were allowed using the Gaussian smearing method and a width of 0.05 eV. The Brillourin zone was sampled with Monkhorst mesh 4×4×1 through all the computational process. The self-consistent calculations apply a convergence energy threshold of 10^{-5} eV. A 15 Å vacuum space along the z direction was added to avoid the interaction between the two neighboring images. The free energy (ΔG) on those catalysts was defined as:

$$\Delta G = E_{DFT} + E_{ZPE} - T \times S$$

where EDFT, EZPE, T and S are the calculation total energy of intermediate on catalysts surface, the zero-point energy, temperature and entropy.

Supporting Figures:

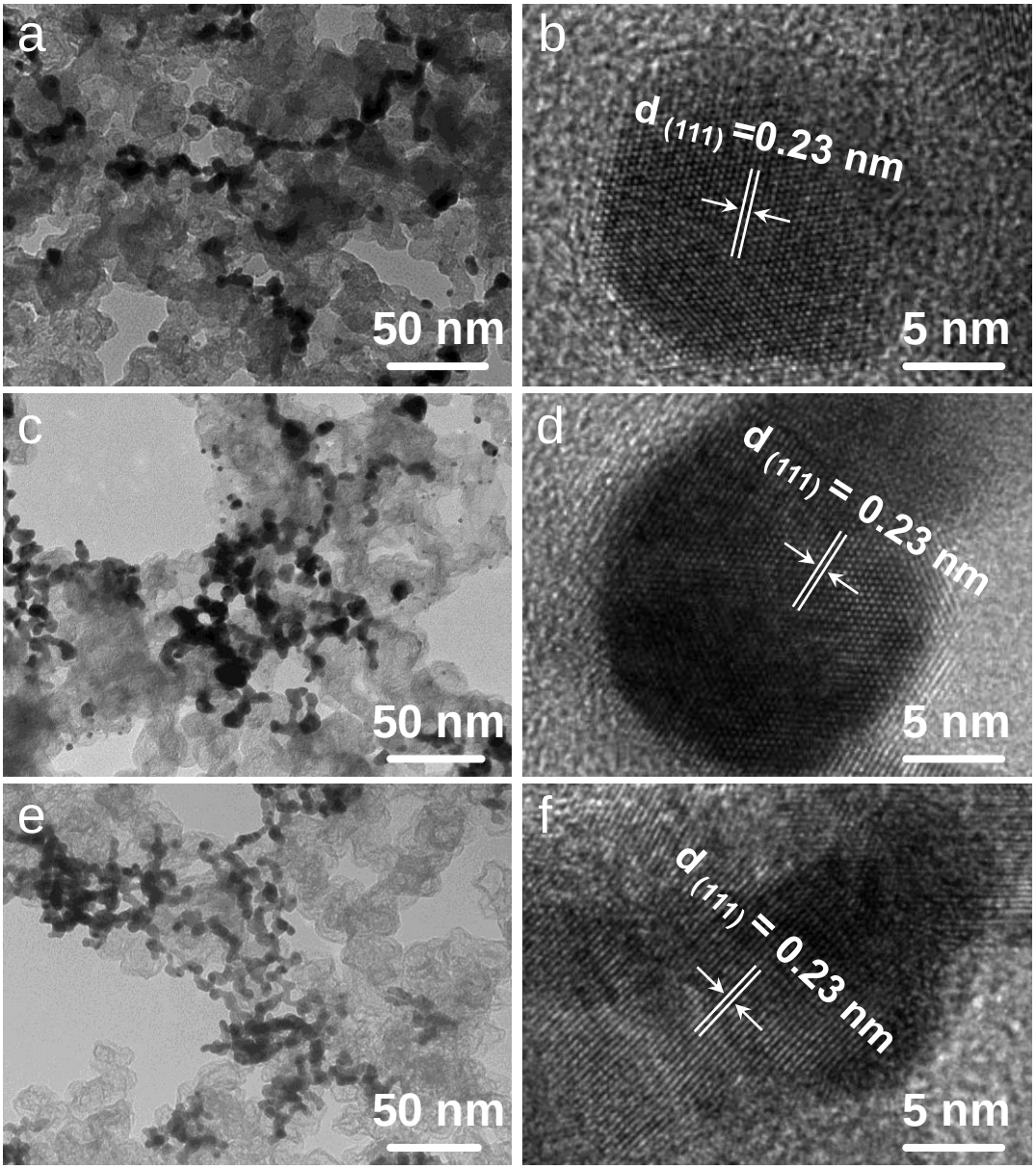

Fig. S1.TEM (a) and HRTEM (b) images of Pd_3Pb IM/C. TEM (c) and HRTEM (d) images of Pd_3Pb IM/LNC. TEM (e) and HRTEM (f) images of Pd_3Pb IM/HNC.

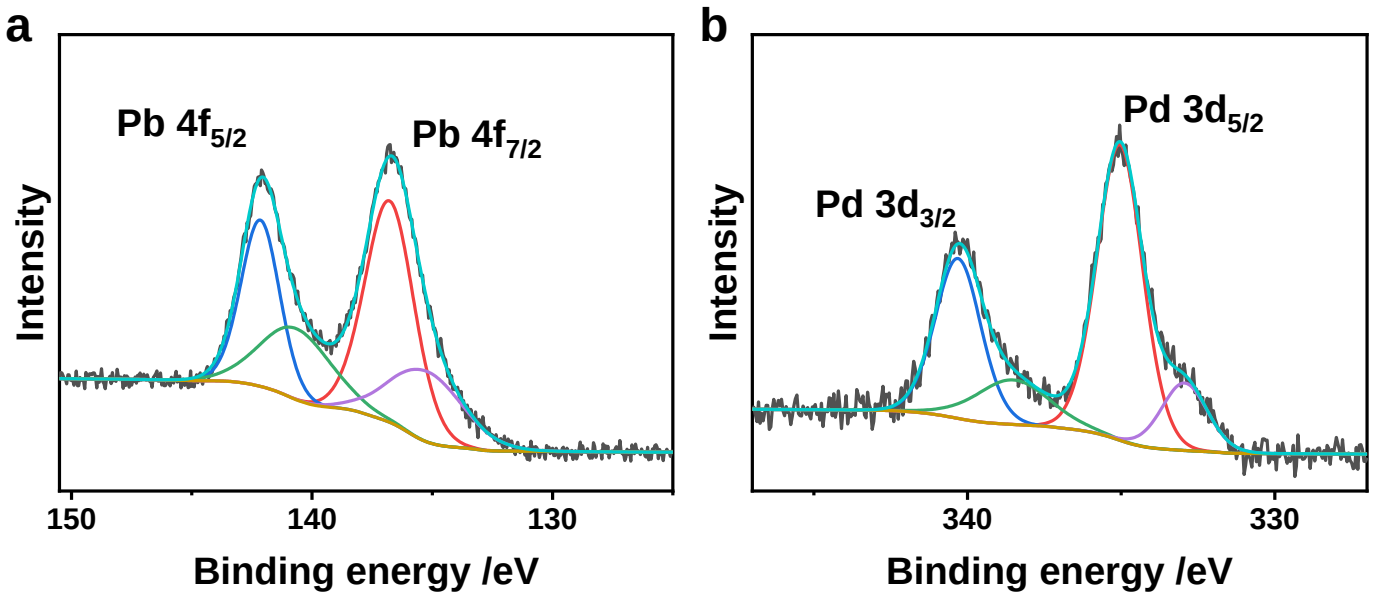

Fig. S2. XPS spectrum of Pd_3Pb IM/C.

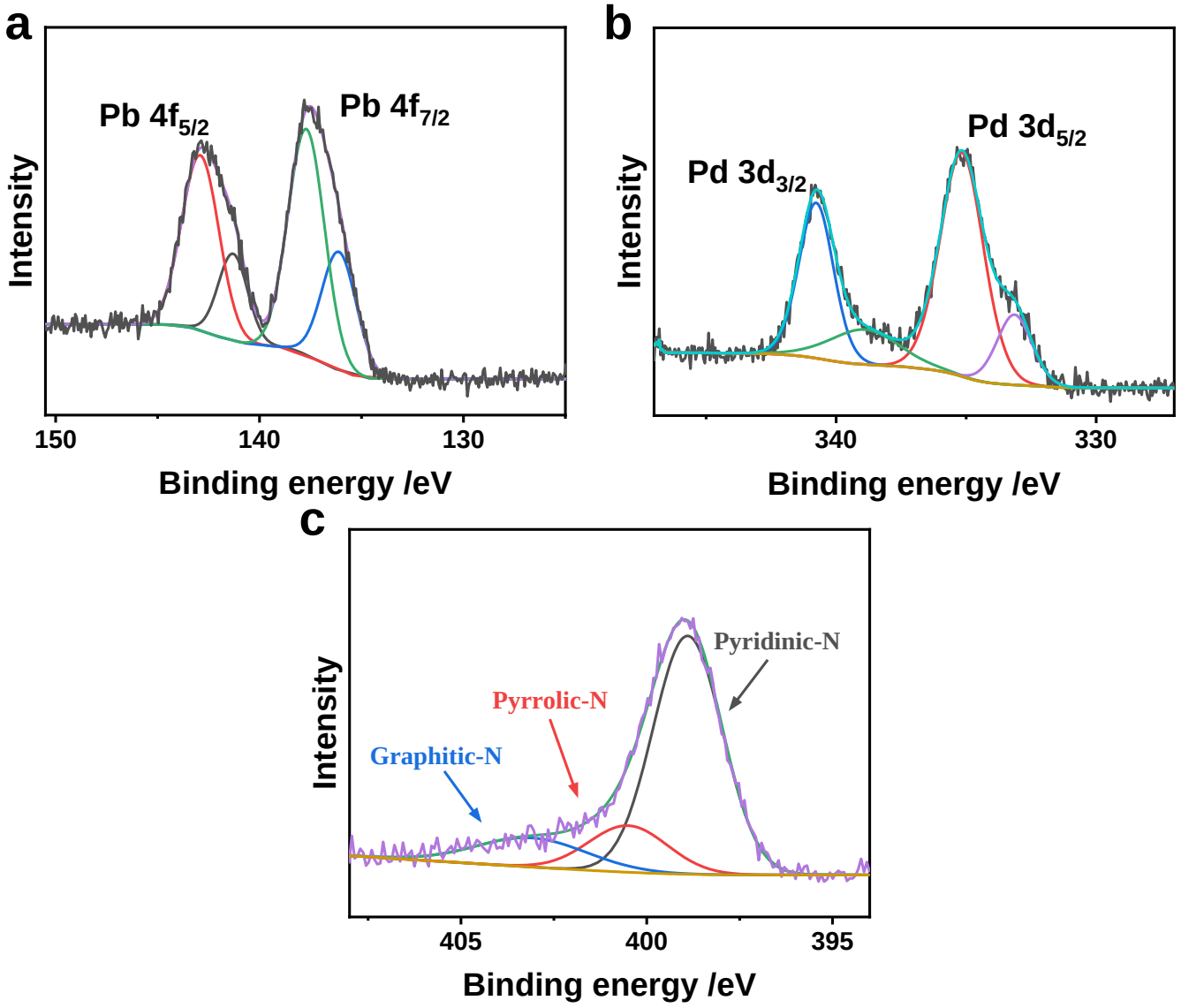

Fig. S3. XPS spectrum of Pd_3Pb IM/HNC.

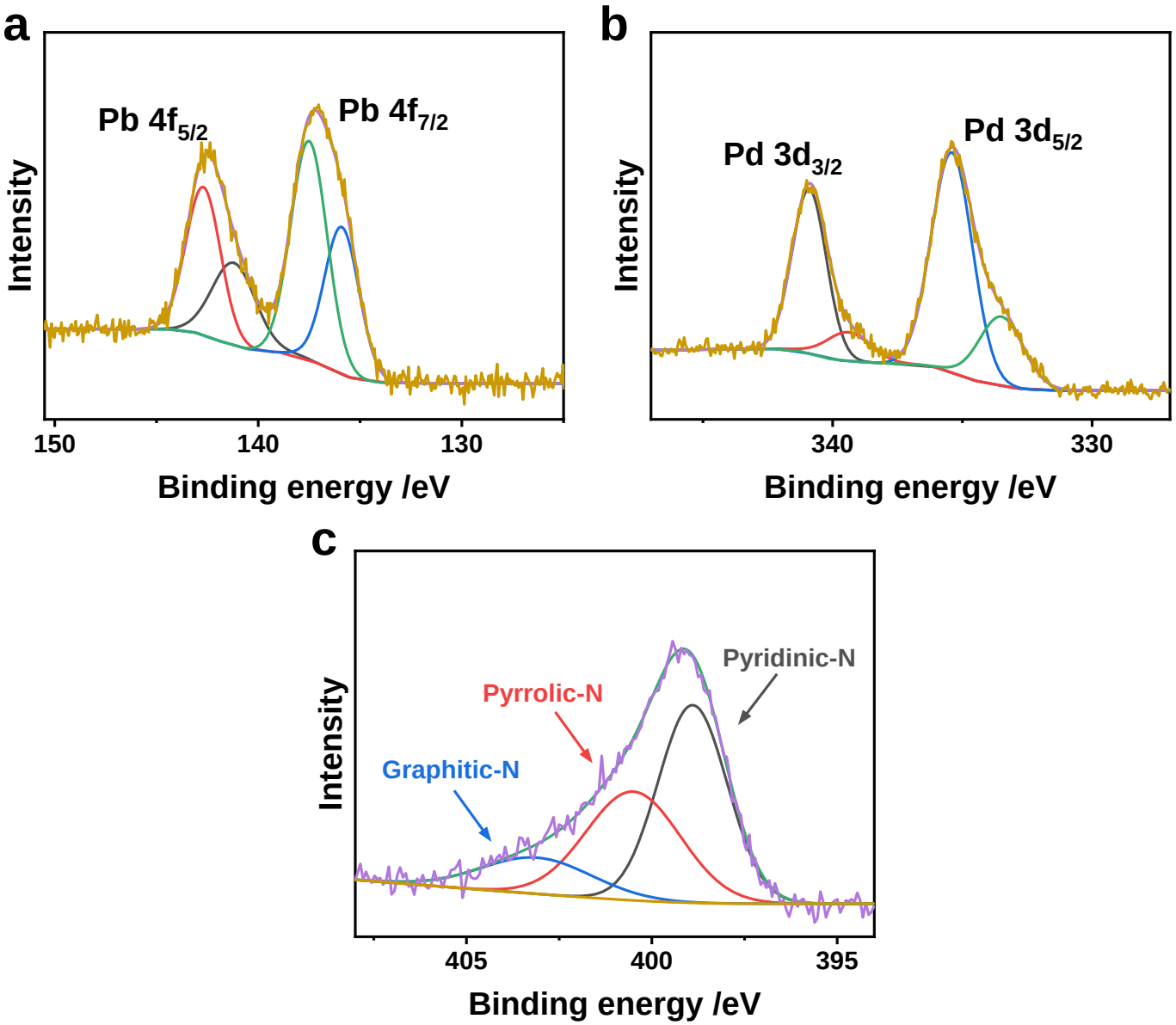

Fig. S4. XPS spectrum of Pd_3Pb IM/MNC.

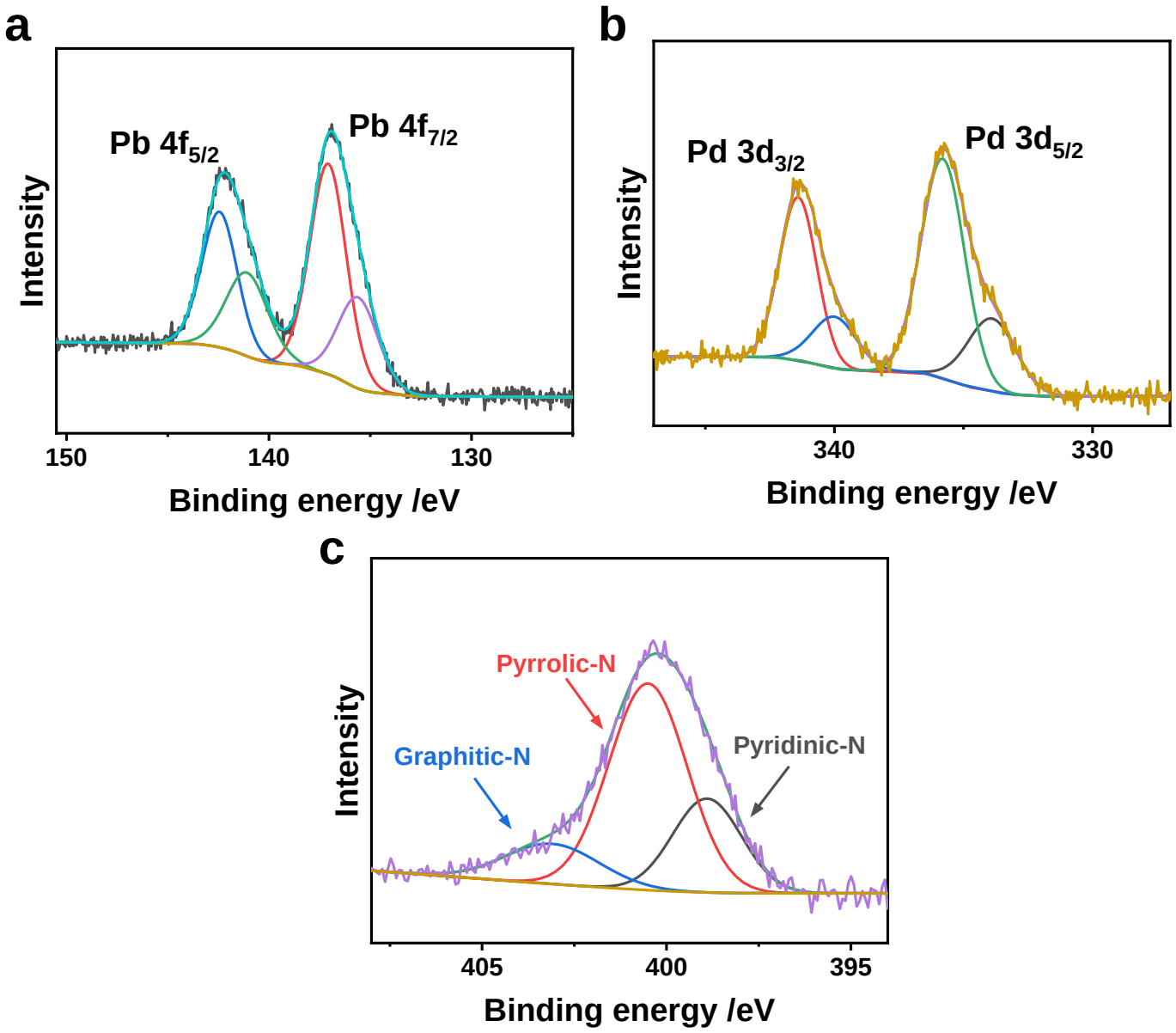

Fig. S5. XPS spectrum of Pd_3Pb IM/LNC.

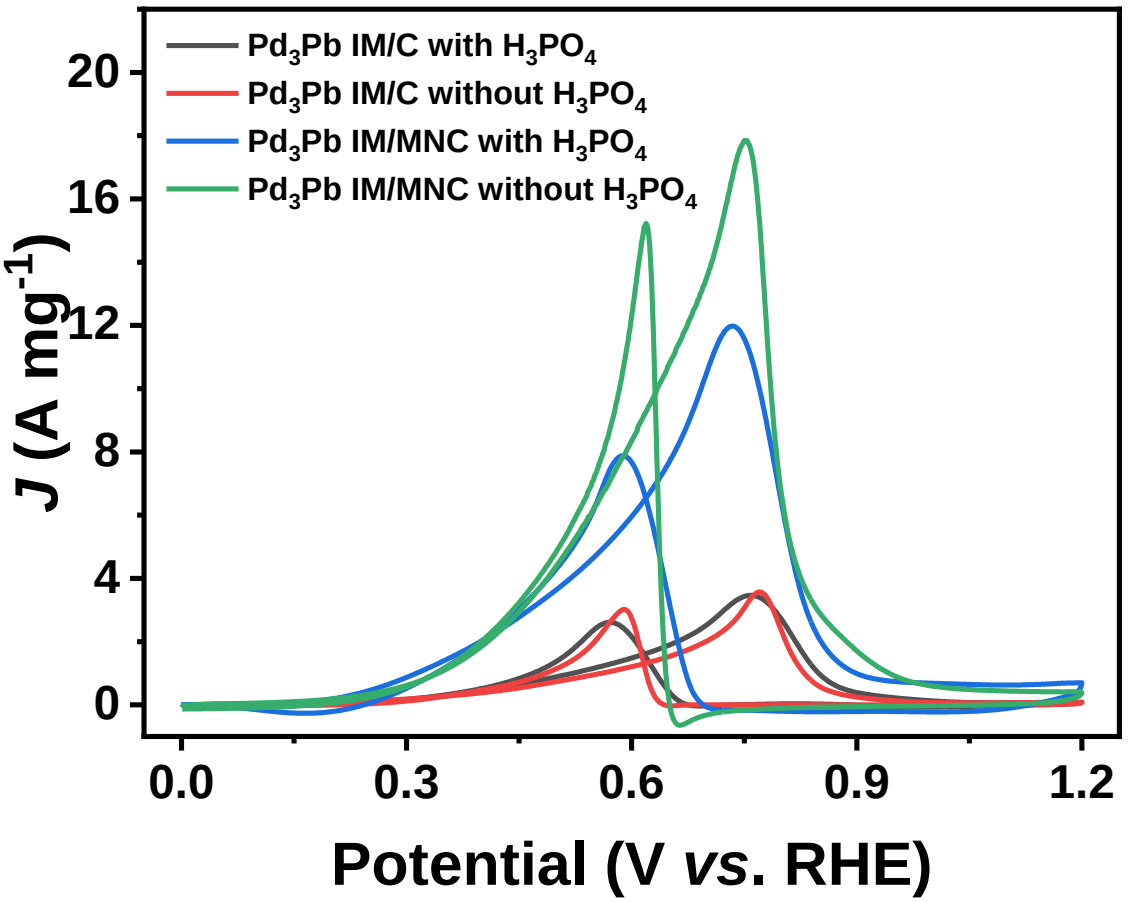

Fig. S6. Control experiment of blocking pyridinic-N.

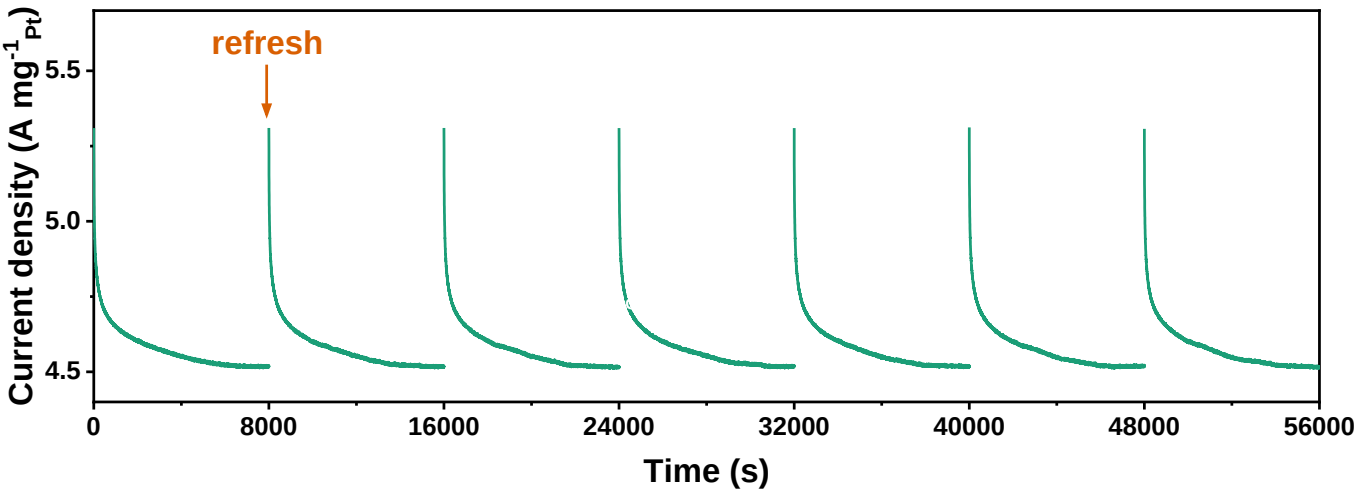

Fig. S7. The 56000 second stability test curve of Pd_3Pb IM/MNC.

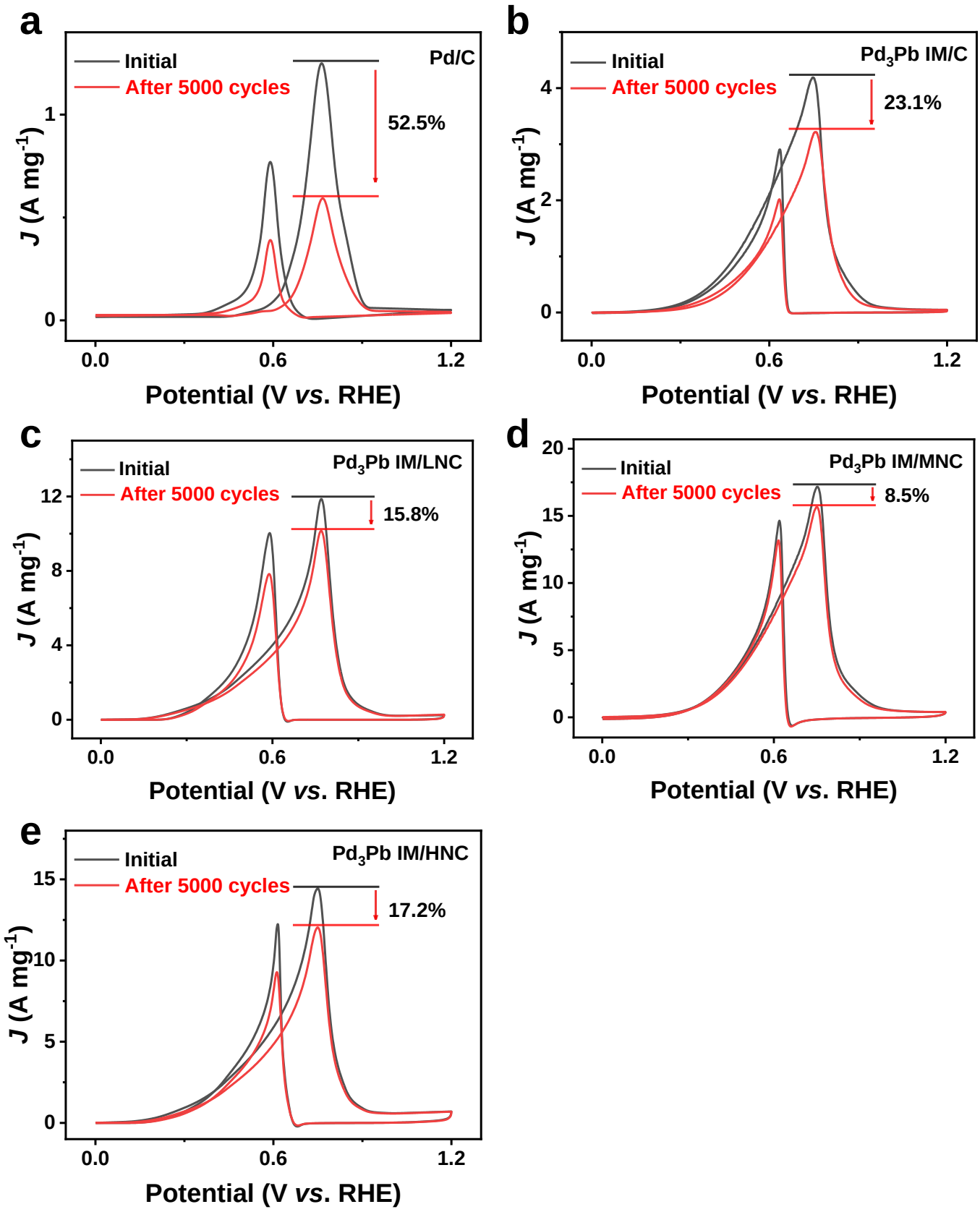

Fig. S8. 5000 CV cycles of synthesized catalysts. (a)Pd/C. (b)Pd_3Pb IM/C. (c) Pd_3Pb IM/LNC. (d) Pd_3Pb IM/MNC. (e) Pd_3Pb IM/HNC.

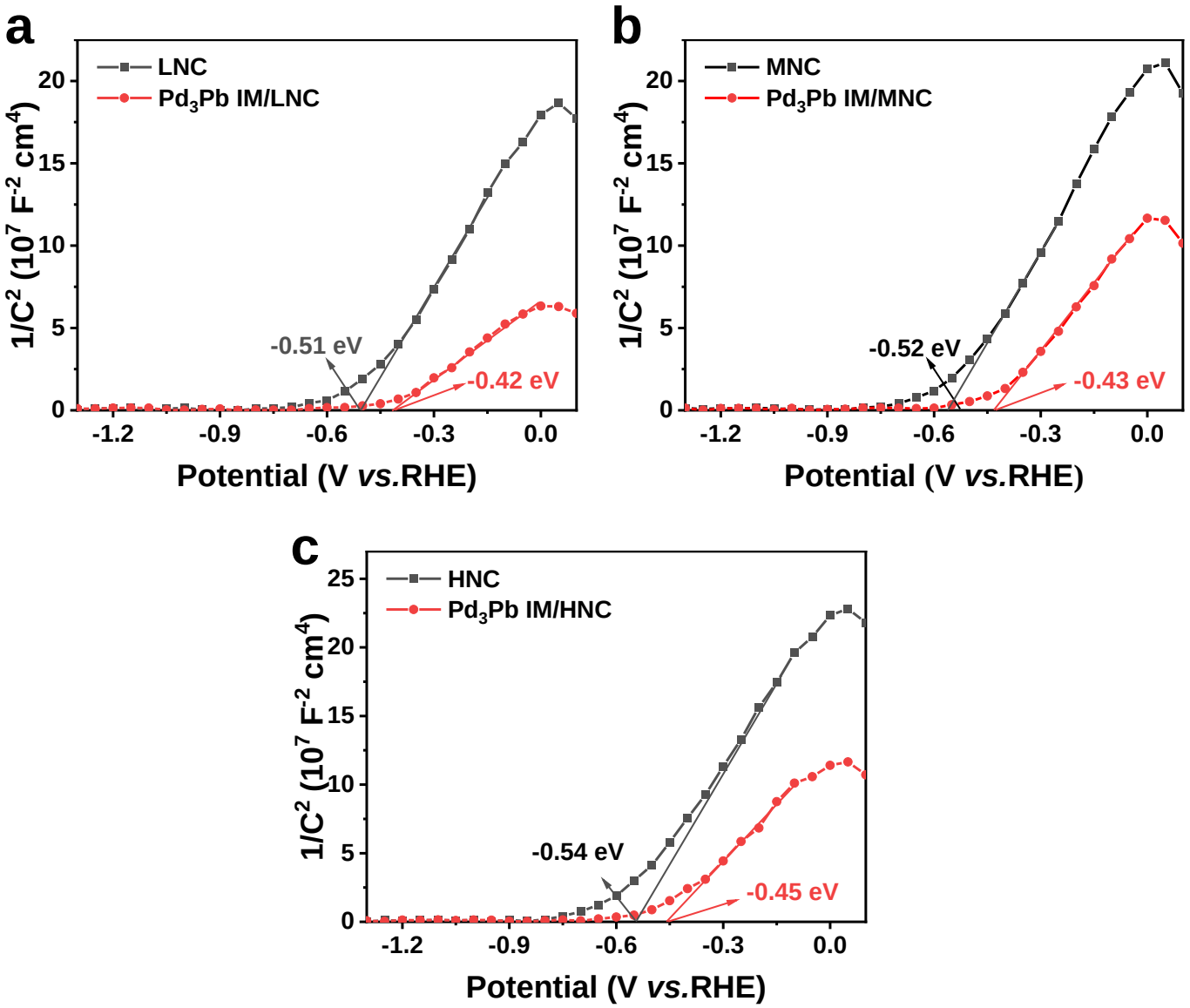

Fig. S9. Motschottky test of synthesized catalysts.

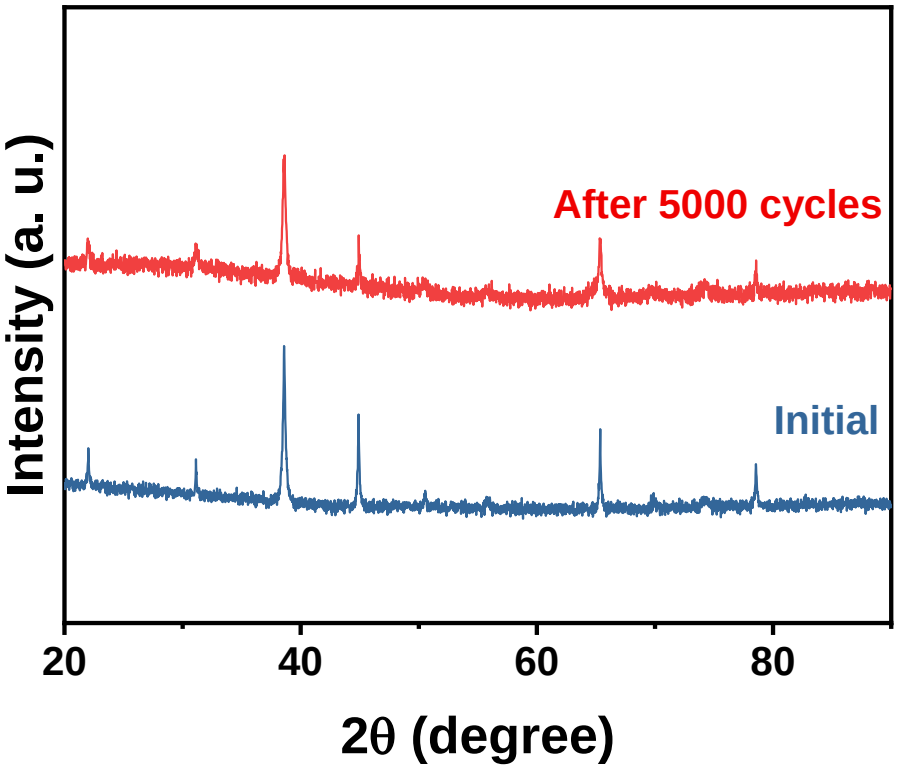

Fig. S10. The XRD pattern of Pd_3Pb IM/MNC after cyclic testing.

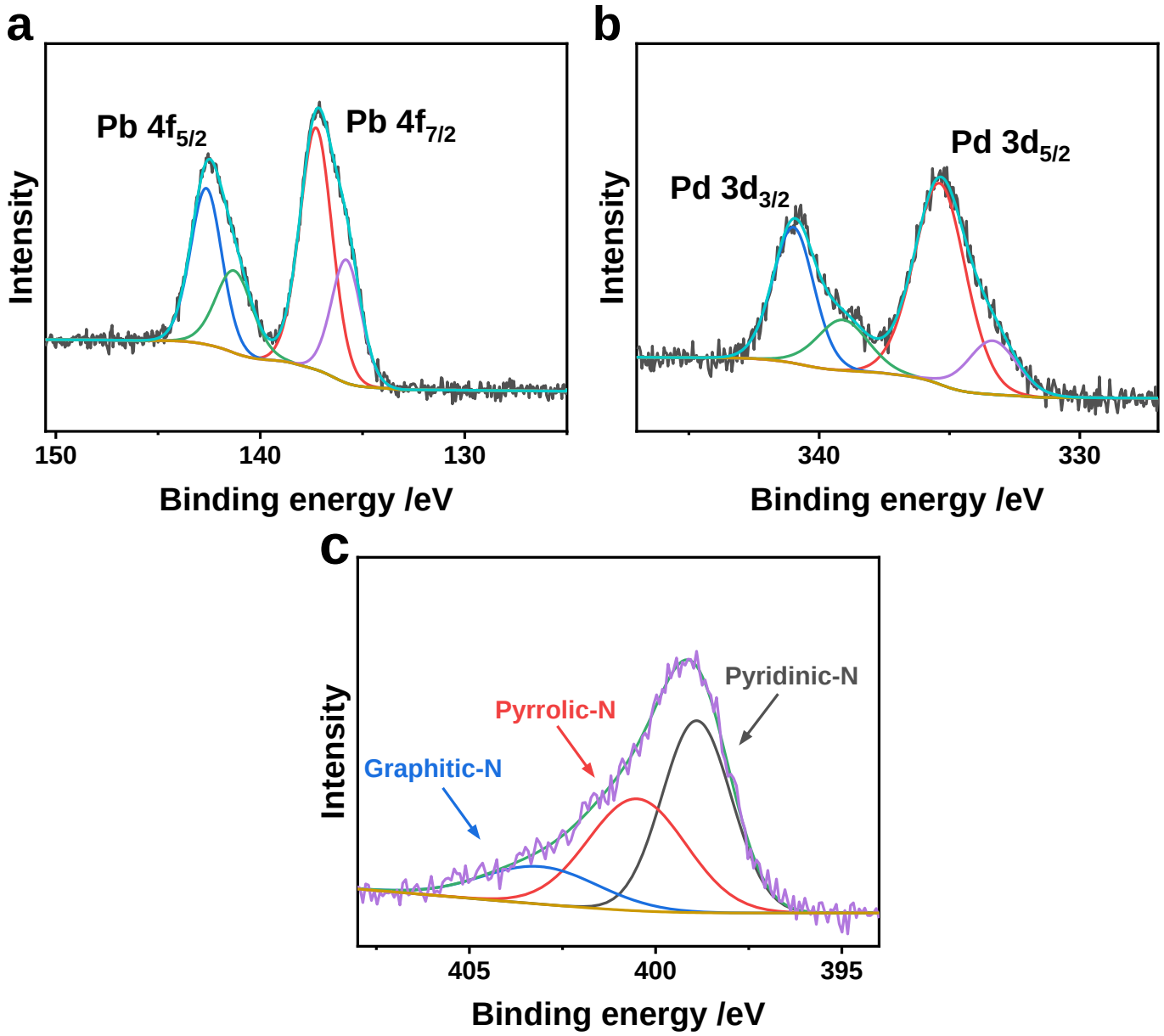

Fig. S11. The XPS of Pd_3Pb IM/MNC after cyclic testing.

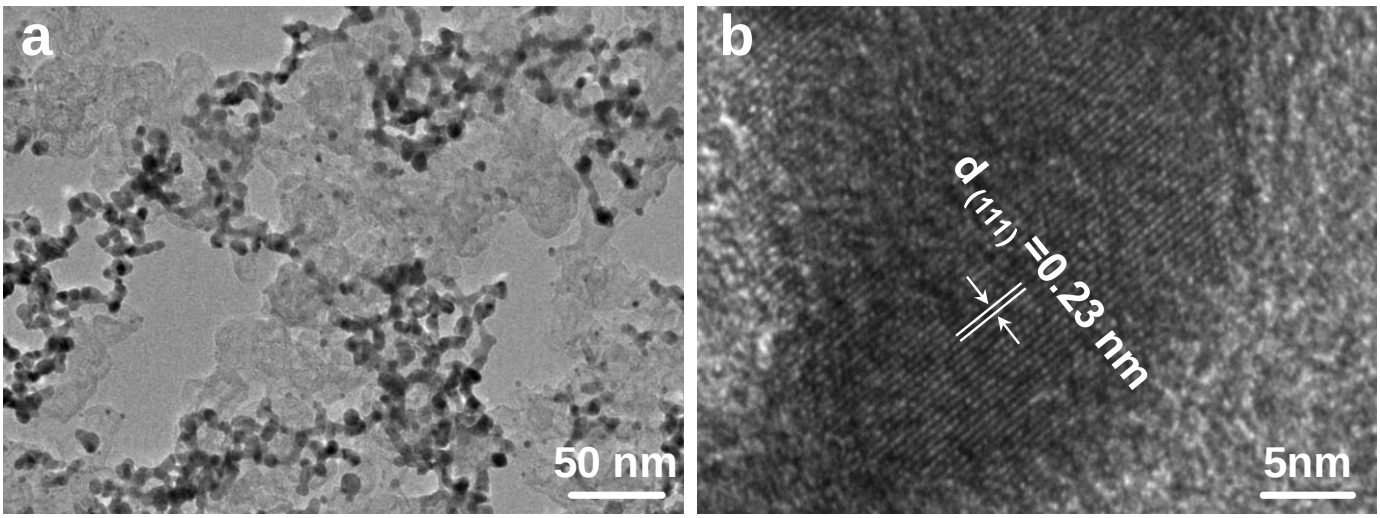

Fig. S12. TEM and HRTEM of Pd_3Pb IM/MNC after cyclic testing.

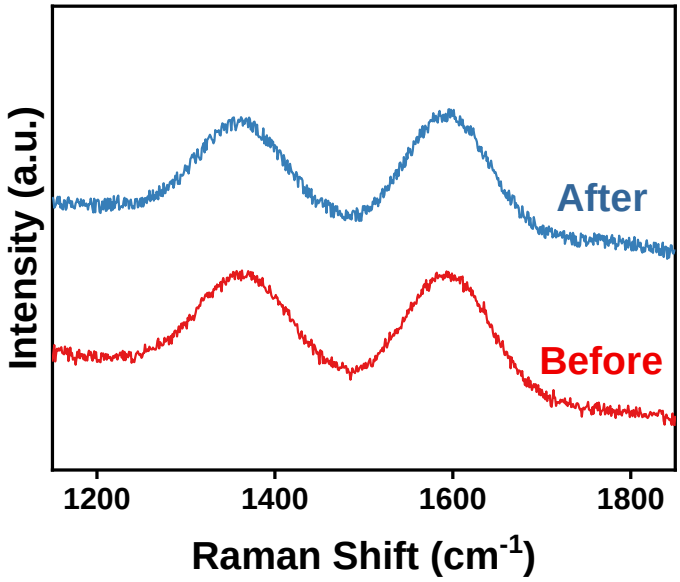

Fig. S13. Raman spectra of Pd_3Pb IM/MNC before and after cycle test.

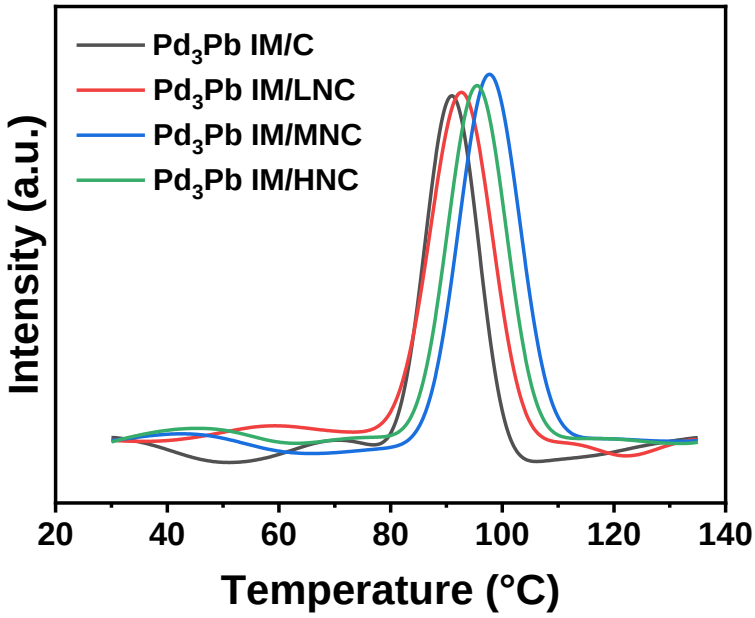

Fig. S14. TPD testing of the synthesized catalyst for CO.

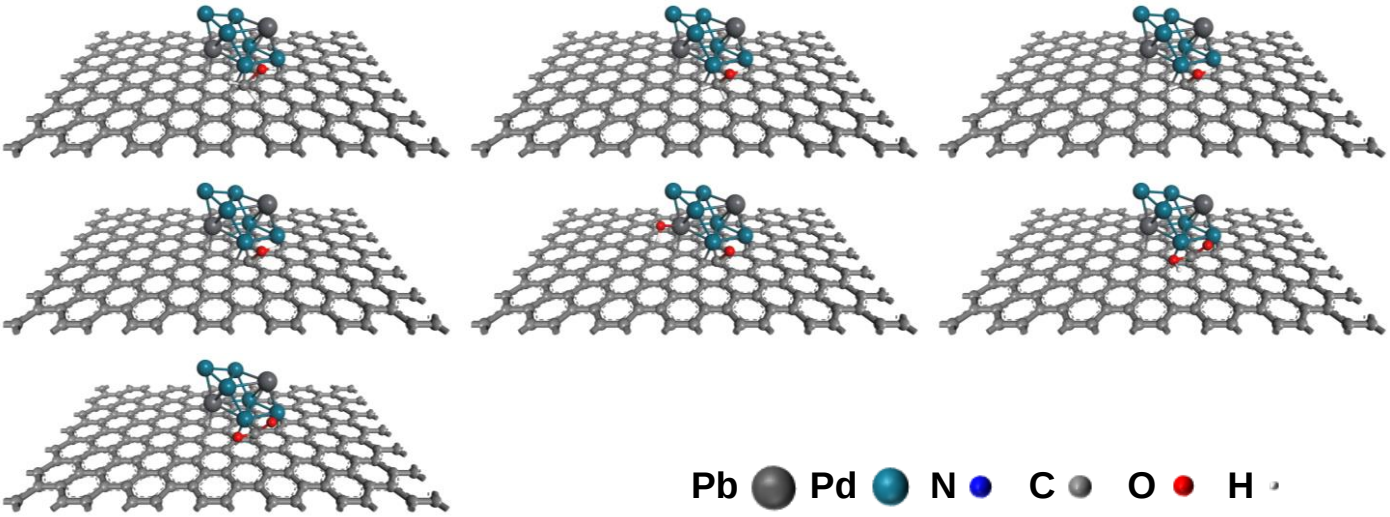

Fig. S15. Scheme of the intermediates involved in MOR catalyzed by Pd_3Pb IM/C model.

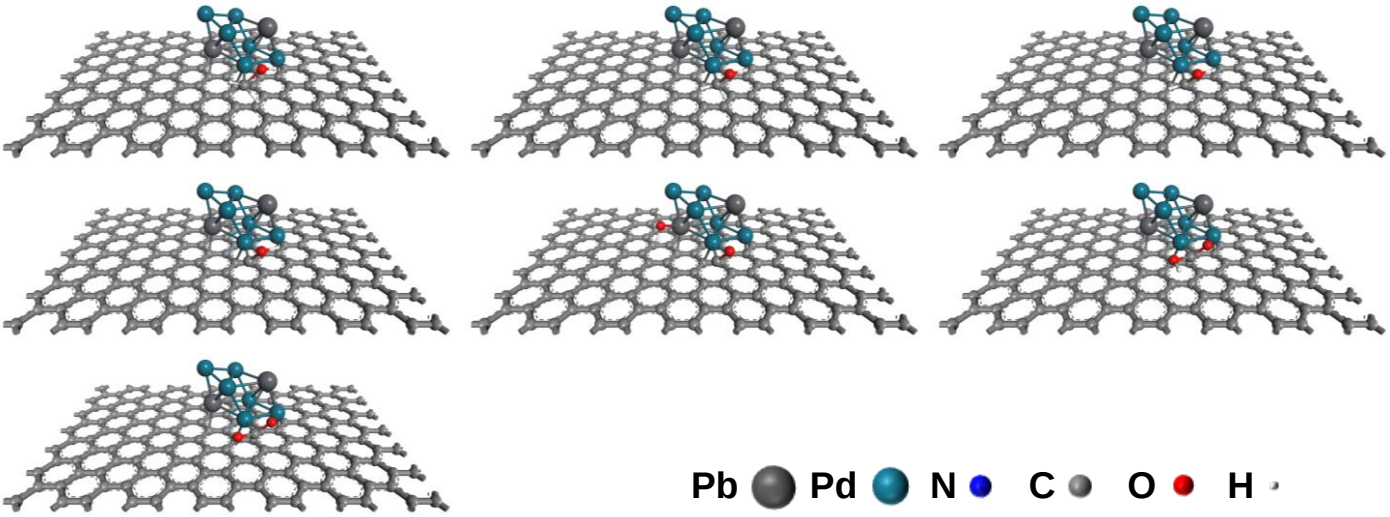

Fig. S16. Scheme of the intermediates involved in MOR catalyzed by Pd_3Pb IM/MNC model.

Table S1. The results of EDS quantitative analysis.

Samples	Atomic ratio / %			
	Pd	Pb	C	N
Pd_3Pb IM/MNC	5.96	1.92	78.58	13.54

Table S2. The specific binding energies of elements in the synthesized materials

	Binding energy (eV)			
Samples	Pd 3d	Pb 4f	pyrrolic-N	pyridinic-N
Pd_3Pb IM/C	142.1	340.3	400.5	403.1
Pd_3Pb IM/LNC	142.7	340.7		
Pd_3Pb IM/MNC	142.5	340.9		
Pd_3Pb IM/HNC	142.2	341.4		

Table S3. The proportion of pyridinic-N to pyrrolic-N.

Samples	Proportion
Pd_3Pb IM/LNC	3.2
Pd_3Pb IM/MNC	1.02
Pd_3Pb IM/HNC	0.43

Table S4. Comparison of the catalytic performances with the representative high performance MOR electrocatalysts in alkaline electrolytes that reported recently.

Catalysts	Electrolyte	MA / A mg^{-1}	SA / mA cm^{-2}	Potential (V vs. REH)	Stability (decay / 100%)	Ref
Pd_3Pb MNC	1.0 M KOH+ 1.0 M methanol	17.83	21.75	0.75	8.5%	This work
PdNW@cCuO_x	1.0 M KOH+ 1.0 M methanol	-	6.17	0.89	10.4%	[1]
Pd_3Sn_2	1.0 M KOH+ 1.0 M methanol	1.3	-	0.85	83%	[2]

CrO_X-Pd/C	1.0 M NaOH+ 1.0 M methanol	2.05	5.3	0.82	12%	[3]
Ptc/$Ti_3C_2T_x$	1.0 M KOH+ 1.0 M methanol	7.32	-	0.34	31%	[4]
Pd_{NPs}/Pd-N_x@C	1.0 M KOH+ 1.0 M methanol	9.45	-	0.79	9.6%	[5]
Pd_3Ni_1-TaN/C,	1.0 M NaOH+ 1.0 M methanol	3.6	-	0.82	12%	[6]
Pd-UNs/Cl-GDY	1.0 M KOH+ 1.0 M methanol	3.6	-	1.09	5%	[7]
PdAgSn/PtBi	1.0 M KOH+ 1.0 M methanol	2.8	4.7	0.9	52.5%	[8]
$PdSn_{0.5}$/Se Ti_3C_2	1 M NaOH+ 1 M methanol	4.7		1.0	14.5%	[9]
Pd_3Pb/$Pt_{2.37}Pb$	1.0 M KOH+ 1.0 M methanol	8.4	13.68		40%	[10]

Table S5. The proportion of pyridinic-N to pyrrolic-N in Pd_3Pb IM/MNC after cycle test.

Samples	Proportion
Pd_3Pb IM/MNC	1.01

Refernces

1. T. Hu, W. Chen, Y. Liu, L. Gong, Z. Jiang, D. Bhalothia, T. Maiyalagan and Z. J. Jiang, *Small*, 2023, **19**, e2304076.
2. J. Xue, Z. Hu, H. Li, Y. Zhang, C. Liu, M. Li, Q. Yang and S. Hu, *Nano Res.*, 2022, **15**, 8819-8825.
3. Y. Qiu, J. Fan, J. Wu, W. Lu, S. Wang, D. Wang, X. Ge, X. Zhao, W. Zhang, W. Zheng and X. Cui, *Nano Lett.*, 2023, **23**, 9555-9562.
4. J. Zhu, L. Xia, R. Yu, R. Lu, J. Li, R. He, Y. Wu, W. Zhang, X. Hong, W. Chen, Y. Zhao, L. Zhou, L. Mai and Z. Wang, *J. Am. Chem. Soc.*, 2022, **144**, 15529-15538.
5. L. Zhuang, Z. Jia, Y. Wang, X. Zhang, S. Wang, J. Song, L. Tian and T. Qi, *Chem. Eng. J.*, 2022, **438**.
6. N. Ye, P. Zhao, X. Qi, R. Zhang, B. Yan, W. Sheng, Z. Jiang and T. Fang, *Appl. Catal. B Environ.*, 2023, **322**.
7. X. Zhang, L. Hui, D. Yan, J. Li, X. Chen, H. Wu and Y. Li, *Angew. Chem. Int. Ed.*, 2023, **62**, e202308968.

8. X. Lao, X. Liao, C. Chen, J. Wang, L. Yang, Z. Li, J. W. Ma, A. Fu, H. Gao and P. Guo, *Angew. Chem. Int. Ed.*, 2023, **62**, e202304510.
9. S. Chen, N. Liu, J. Zhong, R. Yang, B. Yan, L. Gan, P. Yu, X. Gui, H. Yang, D. Yu, Z. Zeng and G. Yang, *Angew. Chem. Int. Ed.*, 2022, **61**, e202209693.
10. X. Wu, Y. Jiang, Y. Yan, X. Li, S. Luo, J. Huang, J. Li, R. Shen, D. Yang and H. Zhang, *Adv. Sci.*, 2019, **6**, 1902249.